Wind turbine noise modeling including aeroacoustic sources and propagation effects : Comparison against field measurements

David Mascarenhas [1]
Benjamin Cotté [2]
Olivier Doaré [3]
IMSIA, UME, ENSTA Paris, CNRS, CEA, EDF, IP Paris
91120 Palaiseau, France

David Ecotière [4]
Gwenaël Guillaume [5]
Cerema, Université Gustave Eiffel, UMRAE
67000 Strasbourg, France

Benoit Gauvreau [6]
Université Gustave Eiffel, Cerema, UMRAE
44340 Bouguenais, France

Isabelle Schmich-Yamane [7]
EDF HYDRO-DTG
France

Fabrice Junker [8]
EDF Renewables
France

ABSTRACT

The study of wind turbine noise and its impact is of growing importance with the increase in the demand for green and clean energy. As it is known that wind turbine noise can be a cause of annoyance in the vicinity of wind farms it is beneficial to predict accurately the generated noise in the design phase itself. A crucial step is the validation of prediction models against field measurements.

[1]david.mascarenhas@ensta-paris.fr
[2]benjamin.cotte@ensta-paris.fr
[3]olivier.doare@ensta-paris.fr
[4]david.ecotiere@cerema.fr
[5]gwenael.guillaume@cerema.fr
[6]benoit.gauvreau@univ-eiffel.fr
[7]isabelle.schmich-yamane@edf.fr
[8]fabrice.junker@edf-re.fr

This article presents a wind turbine noise prediction model that combines Amiet's theory to calculate trailing edge noise and turbulence interaction noise in free field with a wide-angle parabolic equation valid in moving media to account for the long-range acoustic propagation effects. The model considers the wind turbine as an extended noise source and the rotation effects (such as the convective amplification and Doppler effect) are taken into account. The predicted noise levels are compared to those obtained from a measurement campaign where acoustic, meteorological and ground impedance data have been recorded simultaneously. First, the sound source model is validated close to the wind turbines for different wind speeds and directions. Then, noise predictions are compared to Sound Pressure Level measurements at various distances from the sound source, between 350 and 1300 meters.

1. INTRODUCTION

Wind turbine noise impact is one of the main concern that can reduce productivity of wind farms and hence hinders the development of this type of green energy. This leads to the necessity for developing a reliable noise prediction model which is capable of estimating the noise of a wind farm in the design phase itself and correspondingly adapt for desired changes. Various wind turbine noise source models proposed in the literature considers the main sound sources namely turbulent inflow noise (TIN) and trailing edge noise (TEN) [1–3]. The model used in this study is developed on the basis of the one described by Tian and Cotté [2].

To have an understanding of the limits of the wind turbine noise model, simulation results are compared to the field measurements collected in the framework of the PIBE project [4, 5]. In order to isolate the influence of the source, the comparison is done at a reference location defined by the standard IEC 61400-11 (IEC point). The article first describes briefly the experimental campaign and the obtained data [6]. The wind turbine noise model which is based on Amiet's theory for TIN and TEN is then explained and the comparison of the model and the field measurements is shown for a few representative cases.

2. EXPERIMENTAL CAMPAIGN

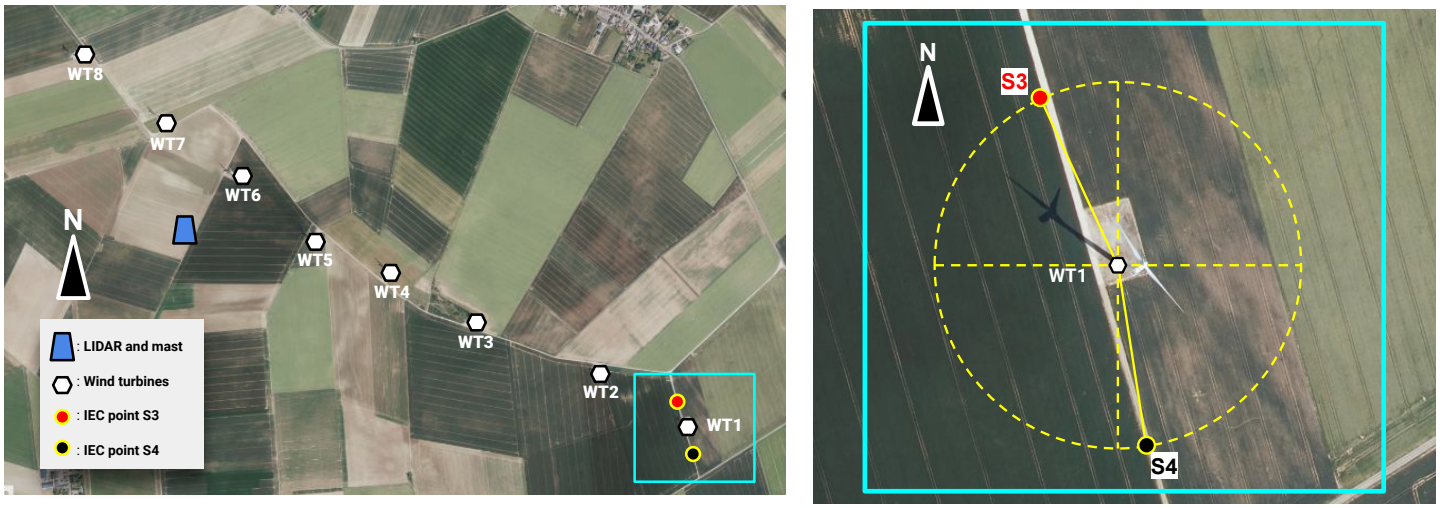

Figure 1: Site map of the studied wind farm (left) and the focused map of the studied wind turbine WT1 (right).

The wind farm is composed of eight 3MW wind turbines of rotor diameter 90m and hub height 80m. The period of intensive observation of the campaign on this wind farm was carried out for 10 days

from 23-06-2020 to 02-07-2020. For this time interval, acoustic data were recorded at the IEC point for two points (S3 and S4) at a distance of 125m from the base of the wind turbine WT1 (Fig. 1). To reduce the influence of the wind-induced noise on the microphone, two wind screens were used (9cm and 50cm diameter) in accordance with IEC 61400-11 recommendations. The relevant acoustic data of the third octave bands measured in 10-minute intervals at S3 and S4 were used to compare with the wind turbine noise predicted by the model. The IEC point S3 was at an angle of 26° and S4 at an angle of -171° relative to the North direction. The LIDAR located near the meteorological mast at a distance of 2.3km away from WT1 simultaneously recorded the data for the wind speed, wind direction, rain, temperature and humidity for heights ranging from 10m to 185m including 85m. The recorded wind direction was found to be majorly between 60° and 120° and between -150° and -60° as can be seen in Fig. 2. A 3D-sonic anemometer placed 80m high on the meteorological mast gave information on the turbulence of the atmosphere at the hub height. The functional data of the wind turbines provided the information of the RPM simultaneously. Since the IEC point is on the ground and relatively close to the wind turbine, the influence of the ground and propagation medium is minimized.

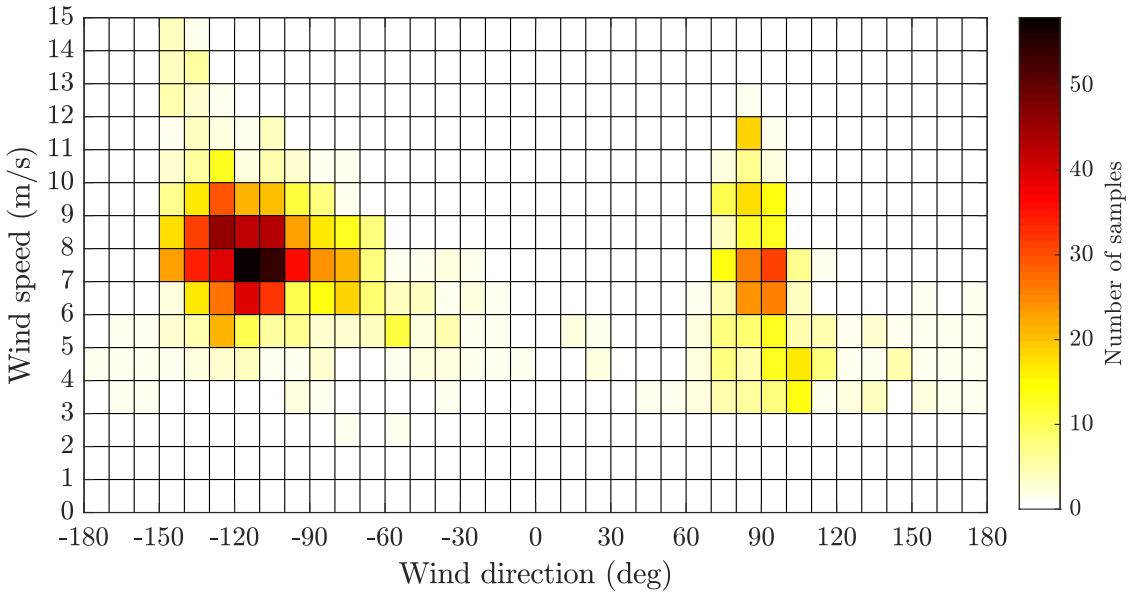

Figure 2: The distribution of the wind speed with respect to the wind direction relative to the north direction over 10 days per 10-min intervals, recorded by the LIDAR at the height of 85m.

3. WIND TURBINE NOISE MODEL

The wind turbine noise model developed by Tian and Cotté [2] predicts the trailing edge noise (TEN) and turbulent inflow noise (TIN) generated by a segmented wind turbine blade based on Amiet's theory. For the TEN, the power spectral density (PSD) observed in the far-field for an airfoil with large span L to chord c aspect ratio ($L > 3c$), is given by [7, 8]:

$$S_{pp}^{\mathrm{TEN}}(x_R, y_R, z_R, \omega) = \left(\frac{kcz_R}{4\pi S_0^2}\right)^2 2L\Phi_{pp}(\omega) l_y\left(\omega, \frac{ky_R}{S_0}\right)\left|\mathcal{L}_{TE}\left(x_R, \frac{\omega}{U_c}, \frac{ky_R}{S_0}\right)\right|^2, \tag{1}$$

where Φ_{pp} is the wall pressure fluctuation spectrum (WPS), l_y is the spanwise correlation length estimated by the Corcos model and $\mathcal{L}_{TE}$ is the transfer function for TEN. In Ref. [2], the wall pressure fluctuation spectrum Φ_{pp} is calculated using Goody's model [9] for the pressure side and

Rozenberg's model [10] for the suction side of the airfoil. Lee developed a new empirical model based on Rozenberg's model that handles flows with higher adverse pressure gradients [11, 12]. Hence the prediction of the trailing edge noise is now used with Goody's model for the pressure side and Lee's model for the suction side of the airfoil.

In the case of the TIN, the radiated acoustic pressure power (PSD) of a large-aspect-ratio airfoil is given by [8, 13],

$$S_{pp}^{\mathrm{TIN}}(x,\omega) = \left(\frac{\rho_0 \omega c z}{2 c_0 S_0^2}\right)^2 \pi U_0 \frac{L}{2} \Phi_{ww}(k_1,k_2) |\mathcal{L}_{\mathcal{TI}}(x,k_1,k_2)|^2, \tag{2}$$

where Φ_{ww} is the 2D energy spectrum of the vertical velocity fluctuations, and $\mathcal{L}_{\mathcal{TI}}$ is the aeroacoustic transfer function. In Ref. [2], the von Karman spectrum Φ_{ww} for homogeneous and isotropic turbulence [13] is used which is based on the velocity fluctuation and the turbulence integral length scale. Using the relation given by Buck et al. (Eq. 7 in [14]) the von Karman spectrum Φ_{ww} reduces to the Kolmogorov spectrum in the inertial range as,

$$\Phi_{ww}(k_1,k_2) = \frac{4}{9\pi}(k_1^2+k_2^2)^{-4/3} \;\; A\epsilon^{2/3} \frac{9\sqrt{\pi}}{55}\left(\frac{\Gamma(1/3)}{\Gamma(5/6)}\right), \tag{3}$$

where A = 1.65 is a universal constant, Γ is the Gamma function, k_1 and k_2 are the turbulent wavenumbers in chordwise and the spanwise direction and ϵ is the turbulence dissipation rate. The integral length scale which is computed from the sonic anemometer measurements requires considerably longer time signal in comparison to the turbulence dissipation rate ϵ. The von Karman spectrum that is dependent on the two parameters of which one is difficult to estimate from sonic anemometer data, is thus replaced by a Kolmogorov spectrum that is dependent on only one parameter and can be easily linked to the field measurements [15]. The change in the turbulence spectra only influences in the far-field Sound Pressure Level (SPL) at frequencies below 1Hz. As the SPL of the TIN is directly proportional to logarithmic of the PSD (eq.2) that is dependent on ϵ (eq.3), the relation of SPL $\propto 6.67 \log_{10} \epsilon$ (dB) hold true. This shows that for an increase in one order of magnitude of ϵ, the predicted SPL is changed by approximately 6.67 dB.

Table 1: Different case studies of the wind speed and wind direction bins. The wind speed and wind direction columns shows the minimum and maximum value of the selected bin and the ϵ and RPM columns show the extremities observed within the respective bin.

Case	τ **(deg)**	**Wind speed (m/s)**	ϵ (m^2/s^3) x10^{-3}	**RPM**	**No. of samples**
1 a	-25, -15	7, 8	2.4, 4.5	12.4, 14.9	9
1 b	-25, -15	8, 9	2.9, 4.7	13.1, 15.7	9
2 a	135, 145	6, 7	1.8, 3.1	10.9, 14	11
2 b	135, 145	8, 9	2.4, 6.0	13.1, 15.7	14
3 a	95, 105	7, 8	3.9, 7.6	11.1, 15.5	30
3 b	95, 105	9, 11	4.3, 12.0	13.4, 14.8	12

4. COMPARISON OF THE MODEL AGAINST FIELD MEASUREMENTS

The data is sorted by wind speed and wind direction bins and the noise prediction is done within the limits of these bins for individual cases. Table 1 summarizes a few cases studies and Fig. 3 to 5 shows the corresponding comparison between the model and the field measurements. From Fig. 3 to 5, the error bars show the standard deviation of the field measurements. The lower curve and upper curve of the shaded area shows the prediction made with the lowest and highest values of the wind speed, ϵ and RPM observed within the respective bin correspondingly.

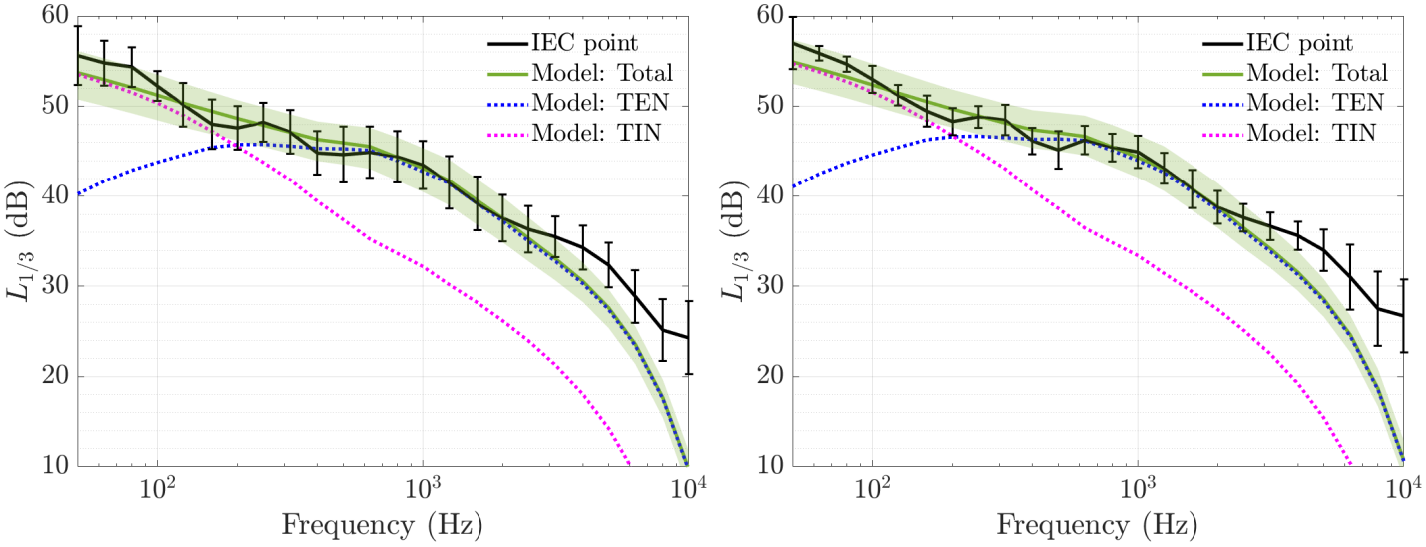

Figure 3: Comparison between the prediction model and the field measurements for the receiver orientation τ=-20±5° and the wind speed bin [7,8]m/s on the left and the wind speed bin [8,9]m/s on the right.

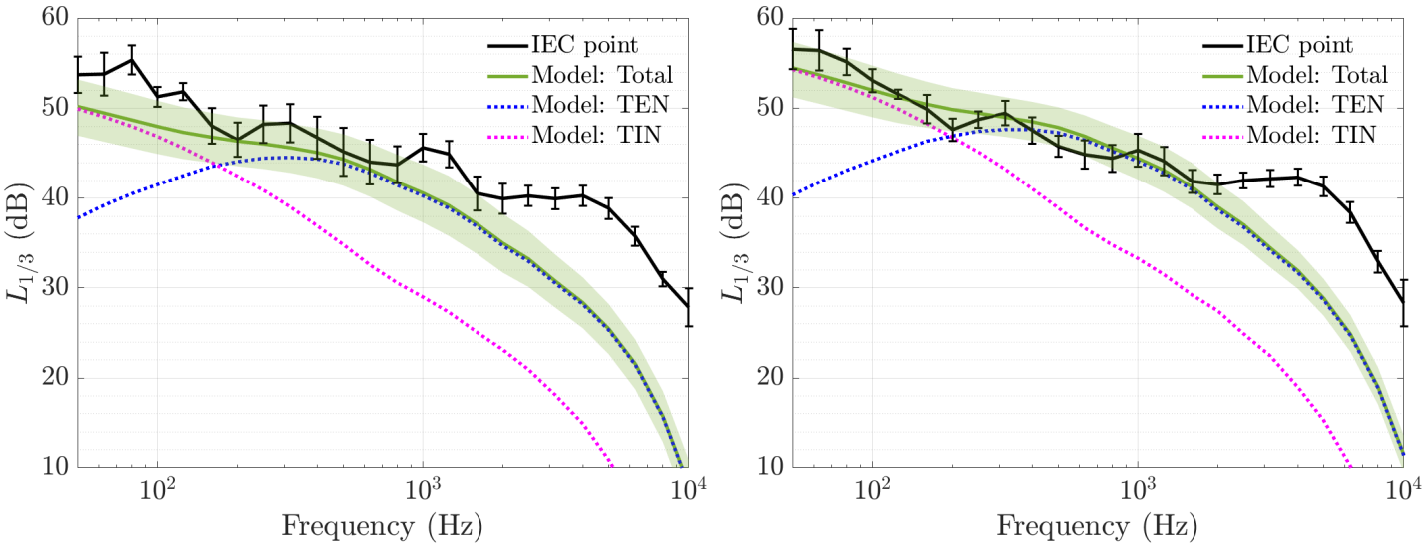

Figure 4: Comparison between the prediction model and the field measurements for the receiver orientation τ=140±5° and the wind speed bin [6,7]m/s on the left and the wind speed bin [8,9]m/s on the right.

From the different cases, it can be seen that the noise prediction model is fairly close to the field measurements. The extremities of the predictions lie within the error of the standard deviation. The

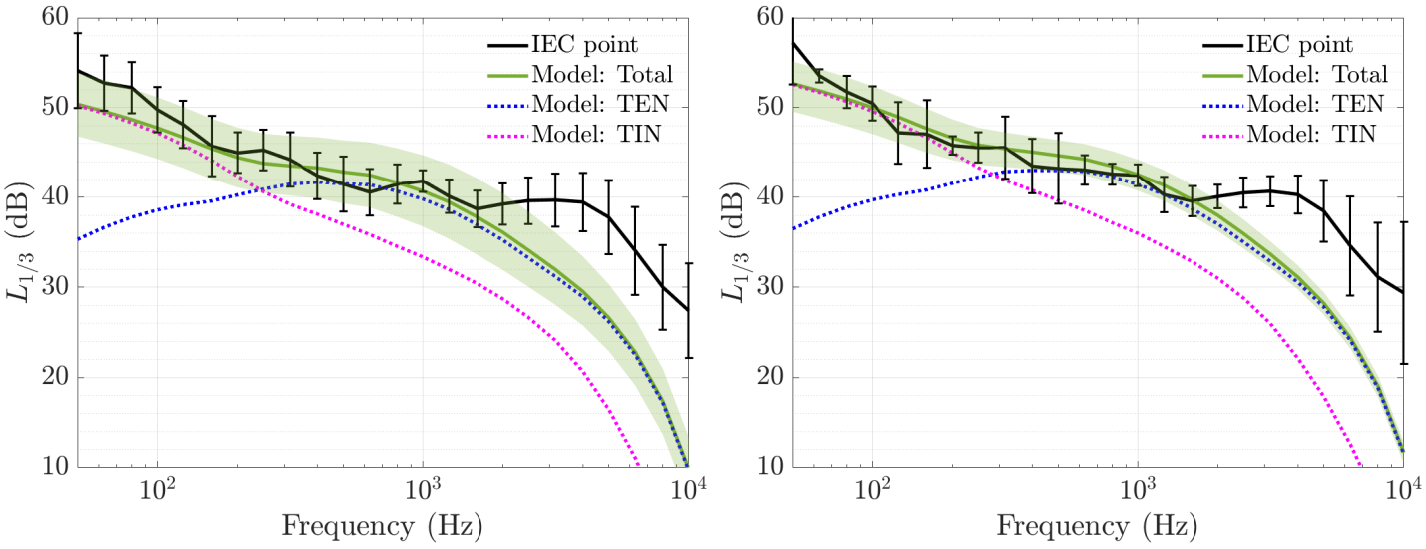

Figure 5: Comparison between the prediction model and the field measurements for the receiver orientation τ=100±5° and the wind speed bin [7,8]m/s on the left and the wind speed bin [9,11]m/s on the right.

frequencies near and above 10 kHz are considered as background noise. The TIN that dominates the lower frequencies is seen to be under-predicted in certain cases because the turbulence dissipation rate is not accurately calculated for the corresponding bin. However, the prominence of the TIN or the TEN at certain orientations of the receiver is well captured by the model. Some peaks around 100Hz and between 2 and 6kHz that are not well predicted may be due to not accounting for certain noise mechanisms such as blade-tower interaction, tip noise etc. The increase in the SPL with the increase in the wind speed is captured by the model which is evident within each case.

5. CONCLUSION

The comparison of the noise model with experimental results shows that the prediction of the individual mechanisms of TIN and TEN are close to the field measurements. The peaks around 100 Hz and 4 kHz are not well predicted which is a limitation of the model. As a perspective, the influence of the noise from the neighbouring wind turbine can also be accounted for better prediction at the IEC point S3. For the prediction of the turbulent inflow noise the important parameter of the turbulence dissipation rate needs to be estimated correctly. On the basis of the turbulence dissipation rate a more accurate prediction can be done for the noise at the IEC point.

Overall, the noise model developed is validated against field measurements and appears to be reasonably good in predicting the third octave band spectra for the turbulent inflow noise and the trailing edge noise. The model can be further developed and used for wind turbine noise studies to predict accurately the soundscape in the vicinity of a wind turbine in operation. As the model itself is physics-based, many practical parameters can be adapted to the desired design of the wind turbine such as the geometry and the blade profile etc. This can be readily extended to estimate the noise levels of the enitre wind farm.

At the conference the comparisons will be presented for long range points that includes the propagation effects with the help of a parabolic equation code in a moving medium [16] along with the effect of the wind shear, as estimated using the LIDAR. The effect of the ground characteristics on the prediction of the noise will also be discussed with the ground acoustic impedance being estimated using an original method [17].

ACKNOWLEDGEMENTS

This project has received funding from the European Union's Horizon 2020 research and innovation program under the Marie Sklodowska-Curie grant agreement No 812719.

REFERENCES

[1] Stefan Oerlemans and J Gerard Schepers. Prediction of wind turbine noise and validation against experiment. *International journal of aeroacoustics*, 8(6):555–584, 2009.

[2] Yuan Tian and Benjamin Cotté. Wind turbine noise modeling based on amiet's theory: Effects of wind shear and atmospheric turbulence. *Acta Acustica united with Acustica*, 102(4):626–639, 2016.

[3] Franck Bertagnolio, H Aa Madsen, and Andreas Fischer. A combined aeroelastic-aeroacoustic model for wind turbine noise: verification and analysis of field measurements. *Wind Energy*, 20(8):1331–1348, 2017.

[4] D Ecotière, B Gauvreau, B Cotté, M Roger, I Schmich, and MC Nessi. Pibe: A new french project for predicting the impact of wind turbine noise. In *Proceedings of the 8th International Conference on Wind Turbine Noise, Lisbon, Portugal*, pages 12–14, 2019.

[5] https://www.anr-pibe.com/en. Accessed on: 25th April 2022.

[6] D. Ecotière, B. Gauvreau, I. Schmich-Yamane, A. Alarcon, M.C. Nessi, F. Junker, G. Guillaume, V. Gary, L. Brendel, G. Litou, R. Boittin, L. Segaud, and H. Lefèvre. A large-scale, long-term experimental campaign for the investigation of wind turbine noise fluctuations and amplitude modulation phenomena. In *Proceedings of the 51st Internoise Congress., Glasgow, UK*, 2022.

[7] Roy K Amiet. Noise due to turbulent flow past a trailing edge. *Journal of sound and vibration*, 47(3):387–393, 1976.

[8] Michel Roger and Stéphane Moreau. Extensions and limitations of analytical airfoil broadband noise models. *International Journal of Aeroacoustics*, 9(3):273–305, 2010.

[9] Michael Goody. Empirical spectral model of surface pressure fluctuations. *AIAA journal*, 42(9):1788–1794, 2004.

[10] Yannick Rozenberg, Gilles Robert, and Stéphane Moreau. Wall-pressure spectral model including the adverse pressure gradient effects. *AIAA journal*, 50(10):2168–2179, 2012.

[11] Seongkyu Lee. Empirical wall-pressure spectral modeling for zero and adverse pressure gradient flows. *AIAA Journal*, 56(5):1818–1829, 2018.

[12] Seongkyu Lee and Jessica G Shum. Prediction of airfoil trailing-edge noise using empirical wall-pressure spectrum models. *AIAA Journal*, 57(3):888–897, 2019.

[13] Roy K Amiet. Acoustic radiation from an airfoil in a turbulent stream. *Journal of Sound and vibration*, 41(4):407–420, 1975.

[14] Steven Buck, Stefan Oerlemans, and Scott Palo. Experimental validation of a wind turbine turbulent inflow noise prediction code. *AIAA Journal*, 56(4):1495–1506, 2018.

[15] Domingo Muñoz-Esparza, Robert D Sharman, and Julie K Lundquist. Turbulence dissipation rate in the atmospheric boundary layer: Observations and wrf mesoscale modeling during the xpia field campaign. *Monthly Weather Review*, 146(1):351–371, 2018.

[16] Vladimir E Ostashev, D Keith Wilson, and Michael B Muhlestein. Wave and extra-wide-angle parabolic equations for sound propagation in a moving atmosphere. *The Journal of the Acoustical Society of America*, 147(6):3969–3984, 2020.

[17] Gwenaël Guillaume, Olivier Faure, Benoit Gauvreau, Fabrice Junker, Michel Bérengier, and Philippe L'Hermite. Estimation of impedance model input parameters from in situ measurements: Principles and applications. *Applied Acoustics*, 95:27–36, 2015.